Published in final edited form as:
J Neurooncol. 2014 December ; 120(3): 489–497. doi:10.1007/s11060-014-1584-1.

Cationic surface charge enhances early regional deposition of liposomes after intracarotid injection

Shailendra Joshi[a,*], **Rajinder Singh-Moon**[a], **Mei Wang**[a], **Durba B. Chaudhuri**[b], **Jason A. Ellis**[d], **Jeffrey N. Bruce**[d], **Irving J. Bigio**[b,c], and **Robert M. Straubinger**[e,f]

[a]Department of Anesthesiology, College of Physicians and Surgeons of Columbia University, New York, NY 10032

[b]Department of Electrical Engineering, Boston University, Boston, MA 02215

[c]Department of Biomedical Engineering, Boston University, Boston, MA 02215

[d]Department of Neurosurgery, College of Physicians and Surgeons of Columbia University, New York, NY 10032

[e]Department of Pharmaceutical Sciences, University of Buffalo, State University of New York, Buffalo, NY 14214

[f]Department of Pharmacology & Therapeutics, Roswell Park Cancer Institute, Buffalo, NY 14263

Abstract

Rapid first pass uptake of drugs is necessary to increase tissue deposition after intraarterial (IA) injection. Here we tested whether brain tissue deposition of a nanoparticulate liposomal carrier could be enhanced by coordinated manipulation of liposome surface charge and physiological parameters, such as IA injection during transient cerebral hypoperfusion (TCH). Different degrees of blood-brain barrier (BBB) disruption were induced by focused ultrasound in three sets of Sprague Dawley rats. Brain tissue retention was then compared for anionic, cationic, and charge-neutral liposomes after IA injection combined with TCH. The liposomes contained a non-exchangeable carbocyanine membrane optical label that could be quantified using diffuse reflectance spectroscopy (DRS) or visualized by multispectral imaging. Real-time concentration-time curves in brain were obtained after each liposomal injection. Having observed greater tissue retention of cationic liposomes compared to other liposomes in all three groups, we tested uptake of cationic liposomes in C6 tumor bearing rats. DRS and multispectral imaging of postmortem sections revealed increased liposomal uptake by the C6 brain tumor as compared to non-tumor contralateral hemisphere. We conclude that regional deposition of liposomes can be enhanced without BBB disruption using IA injection of cationic liposomal formulations in healthy and C6 tumor bearing rats.

[*]sj121@cumc.columbia.edu.

Conflict of interest
The authors declare that they have no conflict of interest.

Keywords

intraarterial; transient cerebral hypoperfusion; focused ultrasound; blood-brain barrier; liposomes; diffuse reflectance spectroscopy

Introduction

Formulation of drugs encapsulated in liposomes can increase their delivery to brain tumors after intravenous injection due to extended circulating half-life of the drug that permits tumor deposition *via* an impaired blood tumor barrier over time [1, 2]. However, few studies have investigated brain tissue uptake of liposomes after a short exposure following the intraarterial (IA) injections. Recently Zhao et al. reported 15-fold greater uptake of magnetically targeted cationic liposomes after IA injection, compared to intravenous injection [3]. We also observed similar advantages of cationic liposomal preparations during IA injection particularly when injected during transient cerebral hypoperfusion (TCH).[4] No study has yet investigated the role of nanoparticle surface charge in relation to deposition efficacy following IA delivery, or the effect of BBB disruption regimens that are under preclinical investigation for enhancing brain delivery.

IA drug delivery is optimal when there is low cerebral blood flow (CBF), high regional uptake, and high systemic clearance [5-7]. In previous studies, we have shown the effectiveness of TCH in improving the IA delivery or pharmacological effects of unencapsulated drugs [8-10]. However, bolus IA injection of liposomal formulations during TCH could confer an additional advantage because there would be minimal contact with blood proteins or liposome-cell interactions [4]. In the present study, the effect of liposome surface charge on brain tissue uptake was investigated by injection of cationic, anionic, and charge-neutral liposomes into the internal carotid arteries of Sprague Dawley rats during TCH, in the absence or presence of varying degrees of BBB disruption mediated by focused ultrasound (FUS). The liposomes were prepared with a non-exchangeable dialkyl indocarbocyanine membrane label [11, 12] in order to permit non-invasive and continuous measurement of liposome concentrations in the brain by diffuse reflectance spectroscopy [13-15]. Having observed significant uptake of cationic liposomes, the IA delivery was tested on C6 glioma-bearing rats.

Material and Methods

Liposome preparation

Dimyristoylphosphatidylglycerol (DMPG), dimyristoylphosphatidylcholine (DMPC), and dioleoyl-trimethylammonium-propane (DOTAP) were purchased from Avanti Polar Lipids (Alabaster, AL). The dialkyl (C_{18}) indocarbocyanine membrane label DiR (Dioctadecyl Tetramethylindotricarbocyanine; $DiIC_{18}(7)$) was purchased from Invitrogen (Carlsbad, CA); and cholesterol (Chol) and other reagents were from Sigma-Aldrich (St. Louis, MO). The three liposome compositions were prepared by the Straubinger laboratory and they contained 5.5: 4.5 (mol:mol) of DMPC:Chol (charge-neutral), or 2.75: 2.75: 4.5 (mol:mol:mol) *X*:DMPC:Chol, where half of the DMPC (*X*) was substituted with either

DOTAP (50% cationic) or DMPG (50% anionic). The final concentration of total dialkyl- plus diacyl lipids for the three preparations was: anionic = 19 mM; cationic = 16 mM; neutral = 23 mM. Liposome-incorporated DiR was quantified by absorbance at 750 nm (Fig. 1a) after dissolution of liposome samples in $CHCl_3$:CH_3OH (vol:vol). Liposome stocks were stored at 4°C under a light-protected inert atmosphere and diluted to the final desired concentration in Tris-saline buffer.

Surgical preparation

These IACUC-approved studies were conducted on 200-300g male Sprague-Dawley rats in accordance with guidelines for the care and use of laboratory animals of the National Research Council of the United States. Details of the surgical preparations are provided in earlier publications [4, 16]. Craniotomy was performed in the right parietal region to enable ultrasonication in Group I and II animals.

C6 tumor implantation

C6 donor cells (American Type Culture Collection, Rockville, MD) were propagated with 1× F-12 media, 10% fetal bovine serum and 200 IU/ml penicillin and 100 μg/ml streptomycin, in a humidified chamber with 5% CO2 at 37°C. Sub-confluent dishes were treated with 0.05% trypsin/0.02% ethylenediamine tetra-acetic acid, and cells were centrifuged. After aspiration of the supernatant, the cells were re-suspended in phosphate-buffered saline and counted. An appropriate amount of phosphate-buffered saline was added to achieve a final concentration of 10^6 cells in 10 μl of Hanks' balanced salt solution that was streotactically injected into the brain at a rate of 1.0 μl/min. After tumor inoculation, the animals were allowed to recover from anesthesia and liposome delivery was tested 1 week later.

Optical measurement of liposome concentration

In-vivo liposomal concentrations were determined by the optical pharmacokinetic (OP) method described by Mourant et al. [15, 17]. The spectral data was processed using Matlab software (MathWorks, Natick, MA) to provide descriptors such as dye concentrations, area under the concentration-time curve (AUC), and end concentration. Because of the time required for injection of the drug using the administration protocol, AUC was calculated for the injection period ($AUC_{injection}$) and the post-injection clearance period ($AUC_{clearance}$). AUC_{total} represents the sum of $AUC_{injection}$ and $AUC_{clearance}$, and is not extrapolated beyond the observed data. In Group 4, post mortem specimens of tumor bearing rats were interrogated by OP and *Hyperspectral imaging* in a manner described in our earlier publication [4].

Focused ultrasound for BBB disruption

In preliminary experiments we investigated the dose requirements for disruption of the BBB by focused ultrasound according to the method described by Yang et al. [18]. The system employed a 3.9 cm diameter transducer (A392S-SU, Olympus NDT Inc., Waltham, MA) with a radius of curvature of 5.6 cm. The FUS transducer was driven by a signal generator (33220A, Agilent Inc., Santa Clara, CA) connected to a radiofrequency power amplifier

(240L, E&I, Ltd., Rochester, NY 14623). Disruption of the BBB was judged by the extravasation of Evans Blue dye (1.4 ml of 1% Evans Blue dye, injected intravenously prior to sonication) and was evaluated 10 min after sonication. Based on preliminary experiments we selected a dose of Definity® ultrasound contrast agent of 50 and 25 μl for Groups 1 and 2, respectively. Thus, the transducer setting and dose of Definity® were identical for all three liposomal preparations.

Transient cerebral hypoperfusion

Previously we have achieved rapidly reversible reductions in CBF in rabbits by carotid occlusion and systemic hypotension induced by two very short acting drugs, adenosine (2-3 mg) and esmolol (2-3 mg) [8, 19]. This technique proved unreliable in normothermic rats, but was effective when core temperature was lowered to ≈32°C. Therefore, hypothermia was employed in conjunction with the TCH regimen for Groups 1 and 2. TCH was achieved in Group 3 by substituting 2 ml of cold (4°C) saline in place of the warm saline used to flush the catheter after esmolol and adenosine administration. This combination decreased the heart rate to 50-80 beats per minute, usually producing a transient sinus pause and a decrease in mean arterial pressure to 10-20 mm Hg. With all three methods, hemodynamic parameters returned to 90% of the baseline values within five minutes of drug injections.

Micro-pulsed delivery of liposomes under flow arrest

To maximize IA drug delivery during TCH, a total volume of 0.6 ml of liposomes, diluted to 1 ml in Tris-buffer, was injected in 12-14 boluses of 70-85 μl every 3 s using a modified micro-injector (Picospritzer III, Parker Hannifin, Pine Brook, NJ) controlled by a signal generator. Fractionation of the injection volume was done to avoid the rapid transit of IA drugs through the cerebral circulation that could have decreased uptake by the brain tissue [20]. The combination of optimum bolus volume and TCH was also aimed to decrease variations in regional concentrations due to streaming [21-23].

Experimental groups

There were four groups of experimental animals, Fig. 2, that all received identical doses of the three different DiR-containing liposome formulations: Group 1 consisted of 18 animals in which BBB disruption was induced by high intensity focused ultrasound; Group 2 consisted of 16 animals in which BBB disruption was induced by lower intensity focused ultrasound; Group 3 consisted of 15 animals that received no ultrasound and received either neutral or cationic liposomes in the same doses as above. Group 4 consisted of 5 C6 tumor-bearing animals for evaluating the delivery of cationic liposomes. CBF and *in-vivo* OP measurements were not undertaken in these animals due to the risk of surgical site bleeding due to tumor implantation. These animals were sacrificed 30 minutes after liposome delivery, to assess the distribution of liposomes using post mortem tissue concentration measurements by OP and MSI.

Data collection and analysis

Physiological data was recorded using a PowerLab 16/35 data acquisition system (ADInstruments, Colorado Springs, CO). For each injection, data were collected at the pre-

injection baseline, at the peak of injection, and 5 and 15 min after liposome injection. The liposome uptake characteristics were described by five parameters: peak concentration, $AUC_{injection}$, the $AUC_{clearance}$ and AUC_{total} periods, and the end concentration. In addition, a retention ratio was calculated as the end injection concentration (15 min after injection) divided by the peak concentration. Statistical analysis was done by repeated measures ANOVA with the post-hoc Bonferroni-Dunn test for multiple comparisons.

Results

The spectral properties of the liposome membrane marker, dialkyl indocarbocyanine probe, DiR, are shown in Figure 1a. The absorption spectrum of this DiR is well separated from the high absorption bands of hemoglobin and deoxyhemoglobin. Fig. 1b-d shows an optical measurement calibration curve obtained from a tissue phantom for DiR-labeled liposome concentrations relevant to *in vivo* concentrations. Good agreement between the known and measured concentrations was obtained for all three liposome compositions. During experiments, 612 spectra were obtained for each injection over a period of approximately 15 minutes (group 1) and 30 minutes (groups 2 and 3).

BBB disruption protocol

We conducted preliminary experiments to optimize the protocol for BBB disruption under a background of propofol infusion and isoflurane anesthesia. The sonication system was similar to one described in the literature by other investigators. In preliminary studies, the acoustic power and concentration of Definity® microbubbles was varied to identify combinations that produced BBB disruption ranging from (*i*) significant, with extravasation of blood cells, to (*ii*) marginal, with subtle extravasation of Evans blue dye and minimal blood cell extravasation. The final conditions selected for consistent grades of BBB disruption based on the extravasation of Evans blue dye required (*i*) 50 μl of Definity®, a pulse length of 50 ms, and a pulse repetition frequency (PRF) of 1Hz, for a total duration of 30 s for high-intensity disruption in Group 1, or (*ii*) 25 μl of Definity®, with all other parameters kept constant for low-intensity disruption in Group 2. The peak-rarefaction pressure at the focal spot of the transducer was measured to be 0.8 mPa and was maintained in both groups. Under the low-intensity conditions, extravasation of Evans Blue could be seen without gross tissue injury. In Group 3 and 4 animals, the BBB was left intact, neither craniotomy nor sonication was undertaken. *Hemodynamic changes* were comparable following IA administration of all three liposomal preparations, within the experimental groups. Significant reductions in heart rate, blood pressure, and CBF (23-33% of baseline) were observed during TCH, that returned to near baseline values by the end of the experiment.

Liposomal deposition with high-intensity focused ultrasound for BBB disruption

For Group 1, which received the most intense FUS application, the peak concentration was highest for the cationic liposomes compared to neutral or anionic liposomes, Table. Representative data for each of the liposome preparations are shown in Fig. 3. Table provides statistics for the liposome treatment groups. Two animals, one receiving anionic liposomes and the other receiving cationic liposomes, did not recover from TCH, and were

eliminated from the statistical analysis. The end tissue concentration of liposomes was 3-10 -fold higher for cationic liposomes compared to anionic and neutral liposomes, and this difference was significant ($p<0.017$). There were also significant differences in the AUC_{total} and in the $AUC_{clearance}$ for cationic vs. anionic and neutral liposomes (Table 1, Fig. 1).

Liposome deposition with low-intensity focused ultrasound

When ranked Group 2 results mirror those of Group 1, except that the pharmacokinetic differences between the three liposomal preparations were more marked, and differences were significant (Table, Fig. 3). Cationic liposomes showed clearly higher peak concentrations, AUCs, and residual tissue concentrations compared to neutral and anionic formulations.

Charge-mediated liposome deposition without BBB disruption

The brain tissue peak concentration was 3-fold greater for cationic liposomes compared to neutral liposomes. The end concentration of cationic liposomes and the area under the concentration-time curve was 7-fold and 9-fold greater, respectively, for cationic liposomes compared to neutral ones (Table, Fig. 3).

Cationic liposome uptake in glioma bearing rats

Fig. 4 shows the hemispheric uptake of cationic liposomes in tumor as assessed 30 minutes after injection in five C6 bearing rats. OP measurements revealed significant retention of liposomes at 30 min after injection. There was no clear evidence of greater uptake by the tumor tissue on multispectral imaging.

Discussion

This study demonstrates the feasibility of achieving regional deposition of nanoparticulate liposomes in brain tissue when injected during states of reduced CBF, and identifies liposome surface charge as a significant determinant of deposition during IA drug delivery in healthy and tumor bearing rats without the need to disrupt the BBB. Peak concentrations, AUC, and end concentrations were 3-15 fold greater with cationic liposomes compared to neutral and anionic liposomes. In contrast to the robust and prolonged tissue concentrations of cationic liposomes, the tissue deposition of anionic and neutral liposomes was minimal and transient.

To increase the propensity for regional drug deposition, we therefore encapsulated the drugs in liposomal formulations, with the rationale that carriers of the appropriate properties could improve the deposition of any drug that could be encapsulated. In a rabbit model, we evaluated the effect of concurrent disruption of the BBB upon brain deposition of a liposomal formulation of mitoxantrone that was optimized for systemic delivery following IV administration [24]. However, that formulation, which was coated with polyethylene glycol to confer extended blood circulation time, did not undergo appreciable deposition during IA delivery. In addition, it appeared that intracarotid mannitol as an agent for BBB compromise resulted in erratic and incomplete disruption of the BBB.[25] We therefore set about developing liposome formulations that were better optimized for brain deposition, and

explored microbubble-mediated disruption of the BBB with focused ultrasound to produce a more consistent disruption of the BBB.

In the present study, we investigated the role of surface charge in mediating brain deposition of liposomes, and optimized conditions to promote deposition. Surface charge mediates cellular interactions of liposomes; both positive and negatively charged liposomes interact with cells more extensively than non-charged liposomes. However, for systemic applications involving IV delivery, high surface charge density results in interaction with serum proteins and rapid clearance. In IA delivery, these constraints are largely eliminated because of the minimal temporal opportunities for liposomes to interact with plasma proteins, and the maximized opportunity to interact with vasculature and tissue. We also developed an injection regimen that involved trains of 12-14 pulses at 3 sec intervals to improve tissue exposure and capillary uptake, while avoiding variations in tissue concentrations due to streaming.[21, 22]

The results of this study show that liposome surface charge has major impact on the regional brain deposition. Despite difference due to craniotomy in Groups 1 and 2 vs. intact skull in Group 3, the superiority of cationic liposomes over the other two formulations clearly was evident irrespective of the state of the BBB permeability. Bolus IA injection of cationic liposomes during TCH could confer additional advantages for regional drug delivery. First, as with any IA injection, liver first-pass effects are nonexistent and larger amounts are conveyed to the target. Second, with concurrent TCH, liposome contact with blood proteins is minimal, thereby protecting the surface charge of the particles and increasing interaction with the negatively charged glycocalyx of the endothelial cells. Third, local delivery could reduce reactions to cationic particles minimize uptake by immunological cells. The increased uptake of cationic liposomes observed in this study is consistent with the larger trend of using positively charged particles to deliver drugs across the BBB [26-28]. For example, neurospecific cell-penetrating cationic proteins can cross the BBB to deliver drug cargos [26, 28]. Protamine, a cationic peptide, has been used similarly to facilitate drug delivery, as has cationic albumin [27].

The biomechanical basis of IA nanoparticle delivery is poorly understood. Ongoing experiments with graded cationic liposomal charge, containing 5, 25 and 50% DOTAP content, show cationic increased charge density effects early retention but the concentration declines such that there is little difference 50 and 25% DOTAP after 30 minutes.[29] During IA delivery the uptake of the particles depends on the probability of adhesion of the particle to the vascular endothelium and the affinity with which it binds to endothelium. This process of adhesion is countered by the hydrodynamic stress that arterial flow generates to displace the particles. The IA delivery of nanoparticles has been explained by Hossain et al in their recent publication and is graphically illustrated in a web video [30]. Similar models are being developed to understand the delivery of nanoparticles to brain tissue considering the concurrent effects of flow changes. Histology of glioma reveals areas of thrombosis, hemorrhage and hypoxia that would suggest increased cerebrovascular resistance and significant hurdles to drug delivery. It is also widely believed that the increased permeability of the tumor vascular bed leads to increased hydrostatic pressure in the core of the tumor and could result in an efflux of drugs and nanoparticles.[31] Such factors pose a challenge to

IA cationic liposome based chemotherapy. Yet the data in Fig. 4 showing hemispheric uptake of liposomes are encouraging. Furthermore the figure provides some evidence of selective uptake of cationic liposomes as compared to the surrounding brain, for at least small tumors. The precise role that IA cationic liposomal chemotherapy will play in glioma therapy remains to be defined. Nonetheless targeted hemispheric liposomal delivery could be used for treating microscopic infiltration by malignant and pre-malignant stem cells so as to prevent remission after surgical excision.

In conclusion, this study demonstrates that it is possible to achieve significant retention of cationic liposomes in the brain and in C6 tumor implants, irrespective of BBB disruption, by employing IA injections during coordinated transient reduction in cerebral blood flow. These results are consistent with, and supportive of, the larger trend to improve drug delivery to the central nervous system with cationic particles/carrier entities and could be used to enhance regional IA chemotherapy of solitary malignant tumors in the central nervous system.

Acknowledgments

This work was supported by grants from the National Cancer Institute at the National Institutes of Health (RO1-CA-127500 and RO1-CA-136843 (S.J.)).

References

1. Straubinger RM, Arnold RD, Zhou R, Mazurchuk R, Slack JE. Antivascular and antitumor activities of liposome-associated drugs. Anticancer Res. 2004; 24:397–404. [PubMed: 15152936]
2. Roy Chaudhuri T, Arnold RD, Yang J, Turowski SG, Qu Y, Spernyak JA, Mazurchuk R, Mager DE, Straubinger RM. Mechanisms of tumor vascular priming by a nanoparticulate doxorubicin formulation. Pharm Res. 2012; 29:3312–3324. doi:10.1007/s11095-012-0823-4. [PubMed: 22798260]
3. Zhao M, Chang J, Fu X, Liang C, Liang S, Yan R, Li A. Nano-sized cationic polymeric magnetic liposomes significantly improves drug delivery to the brain in rats. J Drug Target. 2012; 20:416–421. [PubMed: 22519867]
4. Joshi S, Singh-Moon RP, Wang M, Chaudhuri DB, Holcomb M, Straubinger NL, Bruce JN, Bigio IJ, Straubinger RM. Transient cerebral hypoperfusion assisted intraarterial cationic liposome delivery to brain tissue. J Neurooncol. 2014 doi:10.1007/s11060-014-1421-6.
5. Dedrick RL. Arterial drug infusion: pharmacokinetic problems and pitfalls. J Natl Cancer Inst. 1988; 80:84–89. [PubMed: 3278123]
6. Joshi S, Meyers PM, Ornstein E. Intracarotid delivery of drugs: the potential and the pitfalls. Anesthesiology. 2008; 109:543–564. [PubMed: 18719453]
7. Joshi S, Ornstein E, Bruce JN. Targeting the Brain: Rationalizing the novel methods of drug delivery to the central nervous system. Neurocritical care. 2007; 6:200–212. [PubMed: 17572864]
8. Joshi S, Wang M, Etu JJ, Suckow RF, Cooper TB, Feinmark SJ, Bruce JN, Fine RL. Transient cerebral hypoperfusion enhances intraarterial carmustine deposition into brain tissue. J Neurooncol. 2007
9. Joshi S, Wang M, Etu JJ, Nishanian EV, Pile-Spellman J. Cerebral blood flow affects dose requirements of intracarotid propofol for electrocerebral silence. Anesthesiology. 2006; 104:290–298. [PubMed: 16436848]
10. Joshi S, Wang M, Etu JJ, Pile-Spellman J. Reducing cerebral blood flow increases the duration of electroencephalographic silence by intracarotid thiopental. Anesthesia and analgesia. 2005; 101:851–858. table of contents. [PubMed: 16116003]

11. Meers P, Ali S, Erukulla R, Janoff AS. Novel inner monolayer fusion assays reveal differential monolayer mixing associated with cation-dependent membrane fusion. Biochim Biophys Acta. 2000; 1467:227–243. [PubMed: 10930525]
12. Saito R, Bringas JR, McKnight TR, Wendland MF, Mamot C, Drummond DC, Kirpotin DB, Park JW, Berger MS, Bankiewicz KS. Distribution of liposomes into brain and rat brain tumor models by convection-enhanced delivery monitored with magnetic resonance imaging. Cancer Res. 2004; 64:2572–2579. [PubMed: 15059914]
13. Reif R, Wang M, Joshi S, A'Amar O, Bigio IJ. Optical method for real-time monitoring of drug concentrations facilitates the development of novel methods for drug delivery to brain tissue. J Biomed Opt. 2007; 12:034036. [PubMed: 17614744]
14. Bigio IJ, Bown SG. Spectroscopic sensing of cancer and cancer therapy: current status of translational research. Cancer Biol Ther. 2004; 3:259–267. [PubMed: 15107613]
15. Mourant JR, Johnson TM, Los G, Bigio IJ. Non-invasive measurement of chemotherapy drug concentrations in tissue: preliminary demonstrations of in vivo measurements. Physics in Medicine & Biology. 1999; 44:1397–1417. [PubMed: 10368027]
16. Joshi S. S-MR, Wang M, Chaudhuri D, Straubinger N, Straubinger R, Bigio IJ. The Effectiveness of Transient Cerebral Hypoperfusion Assisted Intra-arterial Delivery of Cationic Liposomes. Journal of Neurosurgical Anesthesiology. 2013; 25:488–489. doi:10.1097/ANA.0b013e3182a4d5ff.
17. Mourant JR, Bigio IJ, Jack DA, Johnson TM, Miller HD. Measuring absorption coefficients in small volumes of highly scattering media: Source-detector separations for which path lengths do not depend on scattering properties. Applied Optics. 1997; 36:5655–5661. [PubMed: 18259392]
18. Yang FY, Fu WM, Yang RS, Liou HC, Kang KH, Lin WL. Quantitative evaluation of focused ultrasound with a contrast agent on blood-brain barrier disruption. Ultrasound Med Biol. 2007; 33:1421–1427. doi:10.1016/j.ultrasmedbio.2007.04.006. [PubMed: 17561334]
19. Joshi S, Wang M, Etu JJ, Pile-Spellman J. Reducing cerebral blood flow increases the duration of electroencephalographic silence by intracarotid thiopental. Anesthesia & Analgesia. 2005; 101:851–858. [PubMed: 16116003]
20. Hardebo JE, Nilsson B. Estimation of cerebral extraction of circulating compounds by the brain uptake index method: influence of circulation time, volume injection, and cerebral blood flow. Acta Physiol Scand. 1979; 107:153–159. [PubMed: 525379]
21. Lutz RJ, Dedrick RL, Boretos JW, Oldfield EH, Blacklock JB, Doppman JL. Mixing studies during intracarotid artery infusions in an in vitro model. J Neurosurg. 1986; 64:277–283. [PubMed: 3944637]
22. Saris SC, Blasberg RG, Carson RE, deVroom HL, Lutz R, Dedrick RL, Pettigrew K, Chang R, Doppman J, Wright DC. Intravascular streaming during carotid artery infusions. Demonstration in humans and reduction using diastole-phased pulsatile administration. Journal of Neurosurgery. 1991; 74:763–772. [PubMed: 1849555]
23. Saris SC, Wright DC, Oldfield EH, Blasberg RG. Intravascular streaming and variable delivery to brain following carotid artery infusions in the Sprague-Dawley rat. J Cereb Blood Flow Metab. 1988; 8:116–120. [PubMed: 3339101]
24. Joshi S, Straubinger R, Wang M, Singh-Moon R, Ergin A, Rai R, Bigio I. Liposomal Mitoxantrone for Intra-arterial Drug Delivery. J Neurosurg Anesthesiol. 2012; 24:491–492.
25. Joshi S, Ergin A, Wang M, Reif R, Zhang J, Bruce JN, Bigio IJ. Inconsistent blood brain barrier disruption by intraarterial mannitol in rabbits: implications for chemotherapy. J Neurooncol. 2011
26. Xia H, Gao X, Gu G, Liu Z, Hu Q, Tu Y, Song Q, Yao L, Pang Z, Jiang X, Chen J, Chen H. Penetratin-functionalized PEG-PLA nanoparticles for brain drug delivery. Int J Pharm. 2012; 436:840–850. doi:10.1016/j.ijpharm.2012.07.029. [PubMed: 22841849]
27. Xia H, Gao X, Gu G, Liu Z, Zeng N, Hu Q, Song Q, Yao L, Pang Z, Jiang X, Chen J, Chen H. Low molecular weight protamine-functionalized nanoparticles for drug delivery to the brain after intranasal administration. Biomaterials. 2011; 32:9888–9898. doi:10.1016/j.biomaterials.2011.09.004. [PubMed: 21937105]

28. Rapoport M, Lorberboum-Galski H. TAT-based drug delivery system--new directions in protein delivery for new hopes? Expert opinion on drug delivery. 2009; 6:453–463. doi: 10.1517/17425240902887029. [PubMed: 19413454]

29. Singh-Moon R. WM, Chaudhuri D, Straubinger N, Straubinger R, Bigio IJ, Joshi S. The Effect of Positive Surface Charge Intensity on the IA-TCH Assisted Delivery of Cationic Liposomes. Journal of Neurosurgical Anesthesiology. 2013; 25:490. doi:10.1097/ANA.0b013e3182a4d5ff.

30. Hossain SS, Hughes TJ, Decuzzi P. Vascular deposition patterns for nanoparticles in an inflamed patient-specific arterial tree. Biomechanics and modeling in mechanobiology. 2013 doi:10.1007/s10237-013-0520-1.

31. Wijeratne NS, Hoo KA. Understanding the role of the tumour vasculature in the transport of drugs to solid cancer tumours. Cell proliferation. 2007; 40:283–301. doi:10.1111/j.1365-2184.2007.00436.x. [PubMed: 17531075]

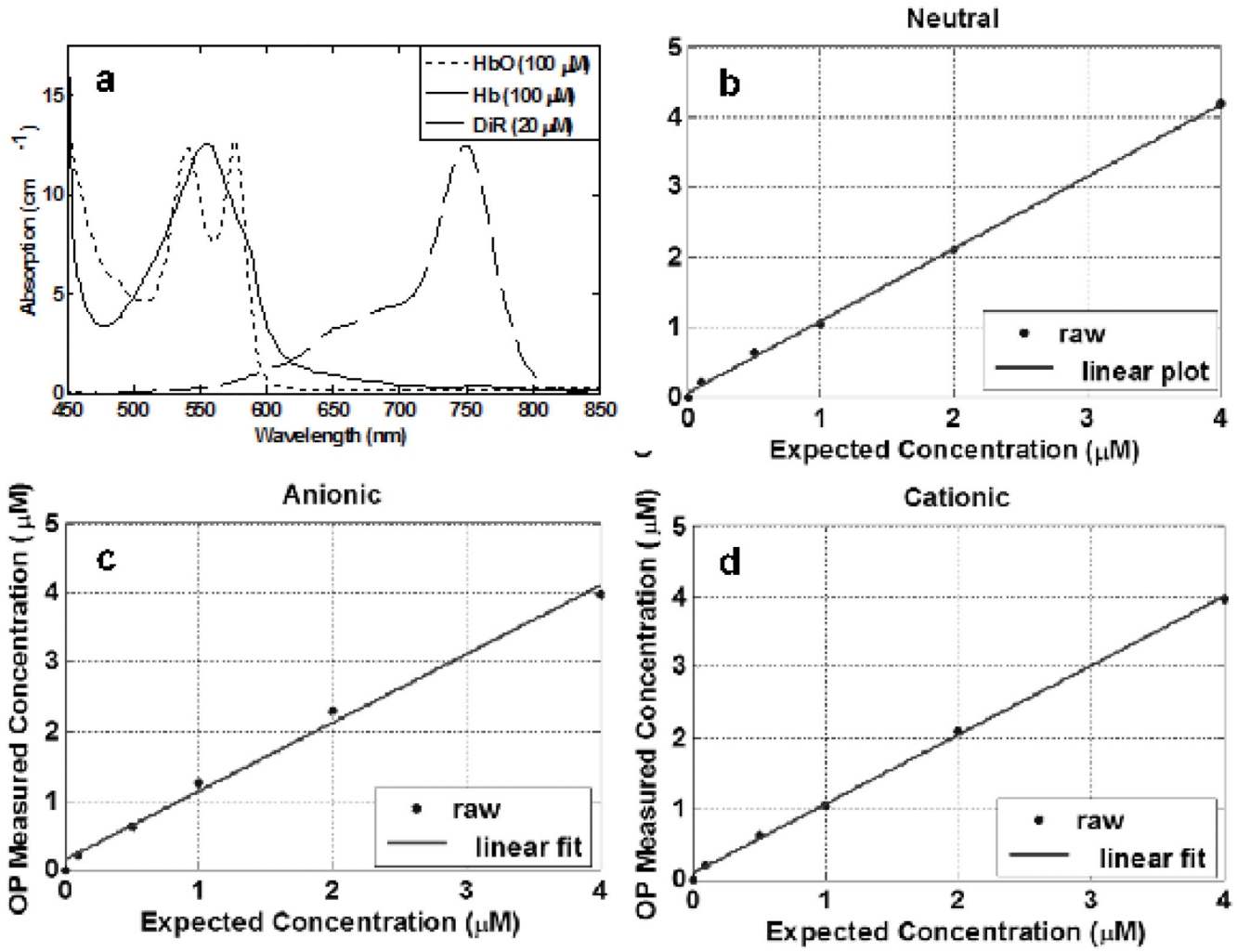

Fig. 1.

(a) The absorption spectra of dominant tissue chromophores, oxy- and deoxyhemoglobin, and liposome membrane label, DiR (Dioctadecyl Tetramethylindotricarbocyanine; $DiIC_{18}(7)$). Plots of expected concentration values vs. OP measured concentrations for known standards of DiR in experimental tissue phantoms are shown for **(b)** neutral, **(c)** anionic, and **(d)** cationic DiR-liposome conjugations.

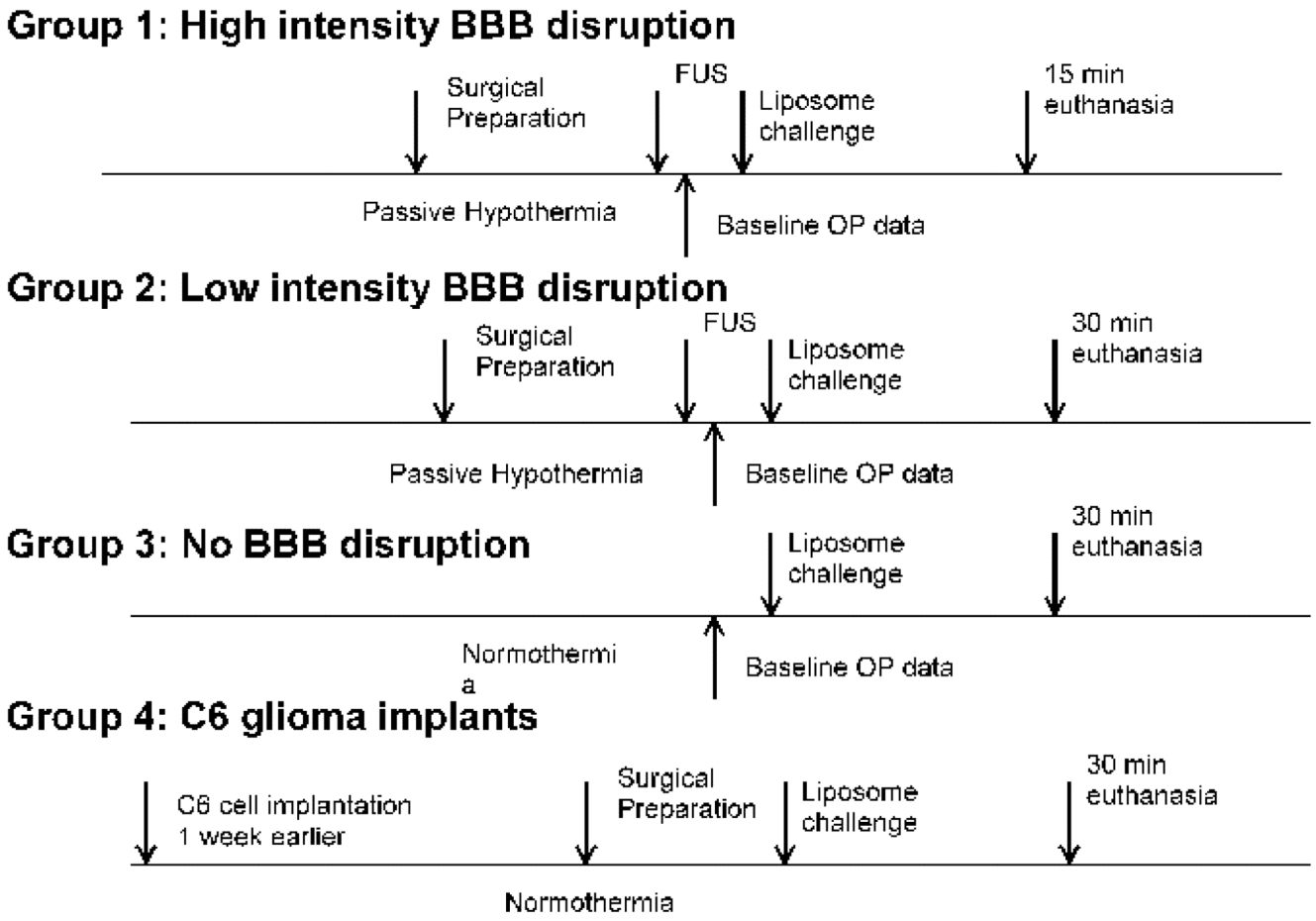

Fig. 2.

Schematic representation of the experimental protocols in the four groups. FUS: focused ultrasound.

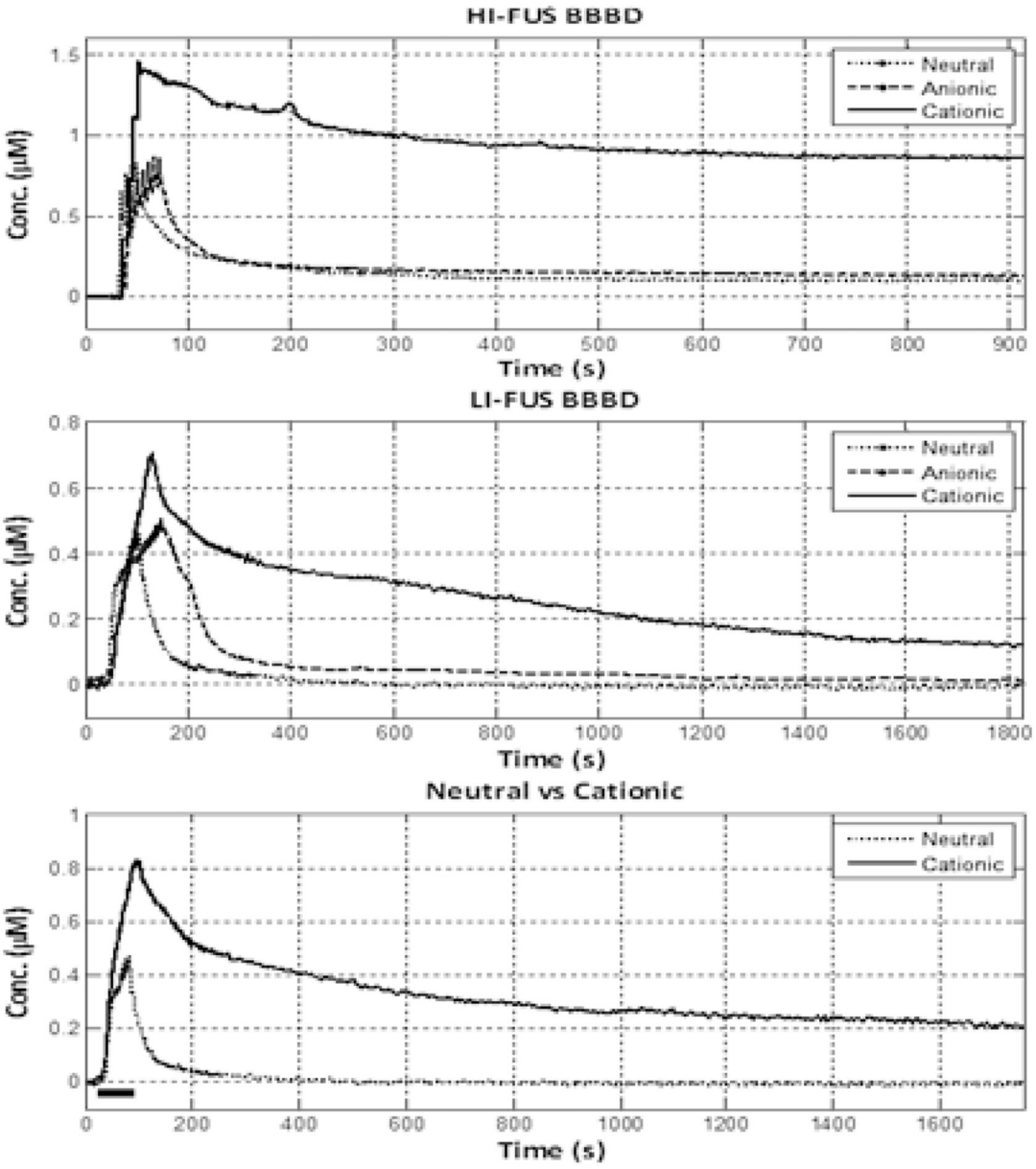

Fig 3.

Vertical panel on right shows representative clearance curves for the three groups. The top row shows representative, liposome pharmacokinetic (PK) data for the group treated with the high-intensity focused ultrasonic blood-brain barrier disruption (HI-FUS BBBD). The middle row shows PK clearance curves for the group treated with low-intensity disruption (LI-FUS BBBD). The bottom row shows representative neutral and cationic liposome PK data for the intact BBB group. Bar indicates intraarterial injection phase period.

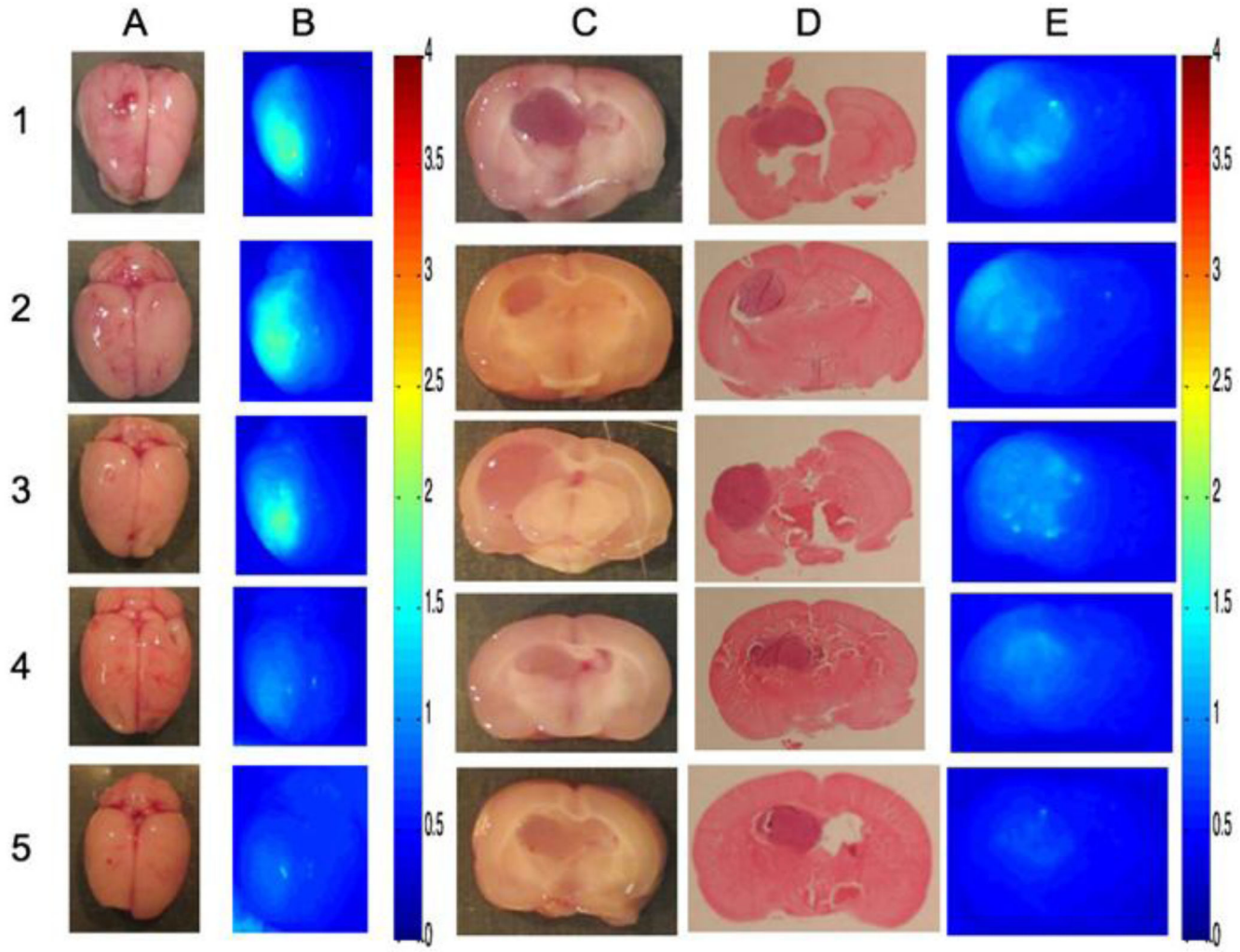

Fig 4.

Uptake of cationic liposomes in five C6 glioma bearing rats (Rows 1-5). Column A: Gross specimen, B: Surface fluorescence with multispectral imaging (MSI), C: Cross section through tumor implant track showing tumor, D: Hematoxylin-eosin staing of the slides, E: Cross-sectional fluorescence with MSI.

Table 1

Tissue concentrations changes with IA liposome injection in Groups 1-4

Tissue concentrations	Cationic	Neutral	Anionic
Group 1: High intensity BBB disruption			
n	**6**	**6**	**6**
Peak concentration (μM)	0.99±0.43	0.75±0.44	0.51±0.20
$AUC_{injection}$ *(μM·s)*	12.9±10.4	16.9±8.07	19.4±6.1
$AUC_{clearance}$ *(μM·s)*	408.3±242.8	129.4±90.7*	52.0±44.8*
AUC_{total} *(μM·s)*	421.2±249.1	146.3±97.8*	71.4±45.4*
End Concentration (μM)	0.41±0.30	0.15±0.08	0.04±0.05*
Retention Ratio (end/peak conc.)	0.40±0.18	0.22±0.06*	0.08±0.08*
Group 2: Low intensity BBB disruption			
n	**5**	**6**	**5**
Peak concentration (μM)	0.72±0.07	0.40±0.12*	0.40±0.07*
$AUC_{injection}$ *(μM·s)*	33.2±8.1	18.9±8.0*	18.6±4.4*
$AUC_{clearance}$ *(μM·s)*	488.1±143.4	18.0±40.5*	39.9±24.7*
AUC_{total} *(μM·s)*	521.3±142.5	37.0±48.6*	58.5±24.7*
End Concentration (μM)	0.15±0.09	0.00±0.01*	0.01±0.02*
Retention ratio (end/peak conc.)	0.22±0.12	−0.02±0.04*	0.04±0.06*
Group 3: No BBB disruption			
n	**8**	**7**	
Peak concentration (μM)	0.83±0.30	0.27±0.09*	
$AUC_{injection}$ *(μM·s)*	41.7±14.4	13.5±3.7*	
$AUC_{clearance}$ *(μM·s)*	597.5±257.3	57.5±11.5*	
AUC_{total} *(μM·s)*	639.3±271.1	70.87±12.6*	
End Concentration (μM)	0.28±0.12	0.04±0.02*	
Retention Ratio (End/peak conc.)	0.34±0.07	0.16±0.09*	
Group 4: Post mortem OP measurements C6 glioma implants			
Side	Ipsilateral (tumor bearing)	Contralateral	
Anterior Cerebral A. (μM)	0.308±0.213	0.035±0.034*	
Middle Cerebral A. (μM)	0.692±0.488	0.010±0.008*	
Posterior Cerebral A. (μM)	0.423±0.331	0.042±0.039*	

*: Significant post-hoc differences between groups 1-3 or sides, group 4